Apoptosis is required during early stages of tail regeneration in *Xenopus laevis*

Ai-Sun Tseng, **Dany S. Adams**, **Dayong Qiu**, **Punita Koustubhan**, and **Michael Levin**[*]
Center for Regenerative and Developmental Biology, Forsyth Institute, and Developmental Biology Department, Harvard School of Dental Medicine, 140 The Fenway, Boston, MA 02115, USA

Abstract

The *Xenopus* tadpole is able to regenerate its tail, including skin, muscle, notochord, spinal cord and neurons and blood vessels. This process requires rapid tissue growth and morphogenesis. Here we show that a focus of apoptotic cells appears in the regeneration bud within 12 h of amputation. Surprisingly, when caspase-3 activity is specifically inhibited, regeneration is abolished. This is true of tails both before and after the refractory period. Programmed cell death is only required during the first 24 h after amputation, as later inhibition has no effect on regeneration. Inhibition of caspase-dependent apoptosis results in a failure to induce proliferation in the growth zone, a mispatterning of axons in the regenerate, and the appearance of ectopic otoliths in the neural tube, in the context of otherwise normal continued development of the larva. Larvae amputated during the refractory stage exhibit a much broader domain of caspase-3-positive cells, suggesting a window for the amount of apoptosis that is compatible with normal regeneration. These data reveal novel roles for apoptosis in development and indicate that a degree of apoptosis is an early and obligate component of normal tail regeneration, suggesting the possibility of the existence of endogenous inhibitory cells that must be destroyed by programmed cell death for regeneration to occur.

Keywords

Xenopus; Tail; Regeneration; Apoptosis; Otolith; Neuron

Introduction

The *Xenopus* tadpole is able to regenerate its tail, including restoration of its nerve, muscle, skin and blood vessel components (Deuchar, 1975). This robust and rapid ability to regenerate the morphology of important tissues has drawn considerable interest as a tractable model for the investigation of this biomedically important phenomenon (Gargioli and Slack, 2004; Ishino et al., 2003; Ryffel et al., 2003; Slack et al., 2004; Sugiura et al., 2004). Regeneration is a complex process possessing a number of distinct phases (Abdel-Karim et al., 1990; Cadinouche et al., 1999; Gardiner et al., 2002). Shortly after amputation and wound healing, an initial swelling gives rise to a regeneration bud, in which proliferating cells rapidly rebuild the tail. This ability is stage-specific, and a non-permissive "refractory" 3-day period (st. 45–47) has recently been identified: when larvae are amputated during this time, regeneration does not take place, although regenerative ability returns immediately afterwards and can be enabled during this refractory period by

[*] Corresponding author. Fax: +1 617 892 8597. mlevin@forsyth.org (M. Levin).

activation of either the BMP or Notch signaling pathways (Beck et al., 2003; Slack et al., 2004).

In the context of efforts to understand biophysical controls of regenerative processes, we investigated the dynamics of cell number control in the regeneration bud. One mechanism by which cell number is controlled during morphogenesis is by programmed cell death (Guha et al., 2002; Saunders, 1966), and apoptosis is involved in sculpting of growing tissue in a number of developmental systems including heart, limb and craniofacial patterning (Bastida et al., 2004; Graham et al., 1996; Guha et al., 2002; Huguet et al., 1999; James, 1994; Nagy et al., 1998), as well as nervous system pruning (Bagri et al., 2003; Erdem et al., 1998; Honig and Rosenberg, 2000; Johnston, 2004; Mallat et al., 2005). Here, we show that despite the massive tissue proliferation required to rebuild the tail, an endogenous early apoptotic event is required for regeneration.

Materials and methods

Scoring of regeneration efficiency

To quantify and compare the regeneration efficiency in drug-treated versus control embryos, we designed a scoring method and introduced a parameter that we called "regeneration index" (RI). Individual embryos within each dish were each scored as follows:

perfect: complete regeneration (regenerated tail, indistinguishable from uncut controls)

good: robust regeneration in presence of minor defects (missing fin, curved axis)

bad: poor regeneration (hypomorphic and defective regenerates)

none: no regeneration.

The percentage of the number of embryos belonging to each category is calculated and then multiplied by 3, 2, 1, or 0, for, respectively, perfect, good, bad and none category. The output is the RI, a value ranging from 0 to 300, with the two extreme values corresponding respectively to no regeneration in any of the embryos and full regeneration in 100% of the embryos in the sample. The RI evaluates the efficiency of regeneration, at the single dish level, of the effect of different treatments and conditions among dishes and versus controls. To compare treatments, a Kruskal–Wallis test, with Dunn's Q corrected for tied ranks, was used on raw scores.

Amputation procedure

Xenopus laevis larvae were grown in 0.1× Marc's Modified Ringers (Sive et al., 2000) supplemented with 10 mg/ml gentamycin (Gibco) and kept at 18°C in 100 mm Petri dishes. At stage (Nieuwkoop and Faber, 1967) 40–41 (pre-refractory), 45–46 (refractory) or 48 (post-refractory), they were anesthetized and placed under a dissecting microscope and tails were amputated using a surgical scalpel blade. The cut was executed at a point just anterior to where the tail begins to taper. Amputated larvae were then distributed into several 100 mm Petri dishes (<30 larvae/dish), each one of them containing the appropriate medium (plain 0.1× MMR/gent or 0.1× MMR/gent+inhibitor). Dishes were kept at 22°C for 6 days (the time necessary to allow control embryos to re-grow a complete tail) without feeding, and then scored.

Inhibitor exposure

The loss-of-function experiments were performed with two apoptosis inhibitors: 2,2′.-Methylenebis-1,3-cyclohexanedione (M50054; Calbiochem #178488) and NS3694 (Calbiochem #178494) at the doses and stages indicated; stocks in DMSO were made at 10

mg/ml. For immediate exposure, larvae were placed into the drug within 5 min of amputation. To terminate exposure, embryos were washed twice in 0.1× MMR. As expected, complete inhibition of apoptosis by the higher doses of either compound induced some curving of the main axis, consistent with the known control of cell number in the extending notochord and neural plate via endogenous programmed cell death (Offner et al., 2005; Van Stry et al., 2004; Yang et al., 1998).

Immunohistochemistry

Spatial detection of apoptosis, proliferation and neurons was performed by immunohistochemistry in whole mount and section. We chose caspase-3 staining as a more specific detector of apoptosis (Chakraborty et al., 2006; Makino et al., 2005; Yu et al., 2002) than classical methods such as TUNEL, which can (and did) give considerable levels of false-positive signal (Stahelin et al., 1998). Briefly, regenerating larvae at the stages indicated were fixed overnight in MEMFA (Sive et al., 2000), heated for 2 h at 65°C in 50% formamide (to inactivate endogenous alkaline phosphatases) and stored at 4°C in PBST (1× PBS+0.1% Tween20)+0.1% NaN$_3$. Immediately prior to staining, they were permeabilized in PBS+0.1% Triton-X 100 for 30 min, blocked with 10% goat serum in PBST for 1 h and incubated at 4°C overnight with primary antibody (anti-activated caspase-3, Abcam #AB13847 for apoptosis (Frankfurt, 1990), anti-phospo-H3, Upstate #05-598 for proliferation, or anti-acetylated α-tubulin, Sigma #T6793 for microtubules) diluted 1:1000 in PBST+10% goat serum. They were then washed 6× with PBST (1 hr each at room temperature) and incubated with an alkaline-phosphatase secondary antibody (Jackson Immunochemicals) at 1:1500 in PBST+10% goat serum overnight at 4°C. After six 1-h washes in PBST, detection was carried out using nitro blue tetrazolium and 5-bromo-4-chloro-3-indoxyl phosphate (X-Phos). Detection was stopped when signal was optimal and background was minimal (usually 6 h at room temperature).

Otolith stain

Larvae at st. 46 (Nieuwkoop and Faber, 1967) were fixed overnight in 4% paraformaldehyde pH 7.5. They were then washed 3× with 1× PBS for 1 min, rocking. Six drops of supersaturated solution of Alizarin Red S were added to 25 mL 0.5% KOH solution. Larvae were then rotated at room temperature in this cocktail for 8 h, washed in methanol and immediately photographed. Ectopic mineralization was also confirmed by viewing samples with a polarizing filter.

Biochemical quantification of apoptosis

Preparation of Freon-extracted lysates: 6–8 frog larvae in minimal liquid were collected, frozen on dry ice and then thawed on ice to prepare lysates. After addition of 200 μl, 15 mM Tris pH 6.8, larvae were crushed with a pestle and vortexed to mix. Two hundred microliters of Freon were added, the sample was then vortexed again and centrifuged at 1000 rpm for 10 min at 4°C. The top layer was removed to a new tube, spun at 1000 rpm for 10 min at 4°C and the top layer was again decanted to a new tube. Protein quantified using the Bio-Rad DC Protein Assay kit to ensure that samples had equal amounts of total protein for the caspase-3 activity assay. One hundred micrograms of protein extract from larvae from each condition were assayed for caspase-3 activity using the Promega CaspACE Assay System Colorimetric kit.

Quantification of proliferation

Larvae processed for immunohistochemistry with H3P as above (at least 4 in each condition) were photographed at the same magnification and the images' brightness level adjusted so that only the positive cells were visible. H3P-positive cells were easily

distinguishable from pigment cells by their color (blue vs. brown) and morphology (dendritic melanocytes vs. small round nuclear H3P stain). A square region, with each side equal to the dorsoventral height of the tail, was positioned with its outer edge touching the distal-most edge of the regenerate. H3P-positive cells were then counted within this region, which encompassed both the regeneration bud and more proximal-tissue. This method of comparing identical tissue areas was necessary because apoptosis-inhibited embryos have no regeneration buds within which cells could be counted.

γ-Irradiation

Total inhibition of proliferation was induced by subjecting intact embryos to 10^4 rads of gamma-irradiation in a Cs^{137} irradiator and raising them as described above.

Results and discussion

We first examined the endogenous pattern of apoptosis in *Xenopus* larval tails by processing them for immunohistochemistry with an antibody to activated caspase-3, a standard marker of apoptosis (Goltzene et al., 2000; Porter and Janicke, 1999; Trindade et al., 2003; Van Stry et al., 2004). Intact larvae at st. 43 possess small numbers of randomly distributed apoptotic cells throughout the tail (Fig. 1A). Six hours post-amputation (hpa) at st. 41, no specific signal was detected near the wound swelling (Fig. 1B). Surprisingly, by 12 hpa, a discrete focus of caspase-3-positive cells was detected in the nascent regeneration bud, both in the overlying epithelium and in the mesenchyme (Figs. 1C, C′, C″). The apoptotic region expanded by 24 hpa (Fig. 1D) and was also present in tails amputated at st. 48 (Fig. 1E), a permissive stage of regeneration occurring after the refractory period. By 48 h, apoptosis could be strongly detected along the extending axis (Fig. 1F). Thus, regeneration in the *Xenopus* tail occurring before or after the refractory period includes a moderate amount of endogenous apoptosis. In contrast, *Xenopus* larvae amputated during the refractory period (Beck et al., 2003; Slack et al., 2004) exhibit a much-expanded region of activated caspase-3 (Fig. 1G, compare to 1D), indicative of extensive cell death throughout the regeneration bud. A high level of apoptosis may be consistent with failure to regenerate during the refractory stage because of loss of cell mass during a process that requires rapid growth.

We next asked whether the endogenous moderate amount of apoptosis was functionally important during regeneration (as opposed to, for example, being a byproduct of amputation damage). We utilized M50054, a specific inhibitor of the activation of caspase-3, which has been shown to prevent cell death, DNA fragmentation and phosphatidylserine exposure in a number of cell types, and to rescue chemotherapy-induced alopecia (death of hair cells) (Tsuda et al., 2001). When larvae were exposed to 20 μM M50054 immediately after amputation, caspase-3 activity was 20%±1% lower in the exposed larvae compared to controls (as measured in an *in vitro* biochemical assay), demonstrating that as expected, caspase-3 signaling was significantly inhibited by M50054 exposure in *Xenopus*. In contrast to control embryos that readily regenerate their tails, larvae exposed to 20 μM M50054 completely fail to regenerate (Figs. 2A, B, quantified in Fig. 2C). The effect was strong and concentration dependent: compared to control embryos (regeneration index 281), those treated with 12 μM or 35 μM of the inhibitor exhibited regeneration indexes that were 107 (reduced by 62%) and 32 (reduced by 88.5%) of the controls, respectively ($N>70$ in all groups, $H=54.7$, $Q>3.286$, $p<0.01$ compared to controls). The same effect was observed when larvae were cut after the refractory period, at st. 48 (50% reduction of RI, $N=41$ and 37 for control and exposed groups respectively, Mann–Whitney test: $U=1316.5$, $Z=6.172$, $p<0.01$), demonstrating that the blockade of regeneration by the apoptosis inhibitor was not stage specific for the pre-refractory time period but indeed applied also to older stages of regeneration.

To ensure that the failure to regenerate was indeed due to inhibition of apoptosis and not a non-specific side-effect of M50054, we confirmed these findings with another apoptosis inhibitor having a different mechanism of action. NS3694 is a diarylurea compound that blocks apoptosome-mediated caspase activation (Lademann et al., 2003). As with M50054, the phenotype was an inhibition of regeneration (Figs. 2A, B) and the effect was strong and concentration dependent (Fig. 2C′). Compared to control embryos (regeneration index 294), those treated with 30 μM or 40 μM of NS3694 exhibited regeneration indexes that were 112 (reduced by 61.9%) and 24 (reduced by 91.7%) of the controls, respectively (*N* for the 40-μM group=29, *N* for the 30-μM group=65; $H=33.9$; $Q>5.25$; $p<0.01$). These results suggest that the up-regulation of apoptosis after amputation is functionally required for regeneration.

Our data (Fig. 1) indicate that apoptosis is normally induced within 12 h of amputation. Thus, we tested the hypothesis that apoptosis is important during the early stages of regeneration by probing the time-dependence of the inhibition effect (Fig. 2D). Larvae exposed to the inhibitor from amputation to 24 hpa exhibited almost the same abrogation (RI=18) of regeneration as observed for exposure that lasted through the entire 7-day period (RI=16). In contrast, embryos that were not exposed to M50054 until 24 hpa, regenerated (RI=288) as well as controls (RI=295). Thus, we conclude that apoptosis during the first 24 h of regeneration is necessary for regeneration.

Interestingly, although the larvae developed normally to st. 49 by the 6-day evaluation period, we observed another phenotype in apoptosis-inhibited larvae. Surprisingly, we observed the appearance of ectopic otoliths, which we describe here to document more fully the embryonic effects of caspase-3 inhibition and illustrate the only other developmental effect of this drug that we could observe (although other subtle changes due to apoptosis inhibition might have gone undetected). Normally, within the otocyst, larvae develop a single pair of mineralized structures known as otoliths (Briegleb et al., 1986; McDiarmid and Altig, 1999; Streeter, 1906) by st. 45 (Fig. 3A). In larvae exposed to either caspase-3 inhibitor from st. 40 to st. 47, ectopic areas of mineralization were detected (Figs. 3B–D) at the lateral edge of the neural tube in 90% of the embryos (*N*=63), and sometimes in other tissues as well (no changes were observed in the endogenous otoliths). One possibility is that programmed cell death normally prevents the formation of these ectopic mineralized structures. It is also possible that this is an unrelated effect of the inhibitor compounds, although we consider it unlikely because it occurs following the application of either of the blockers (which have different mechanisms of action but have in common their blockade of programmed cell death).

To gain insight into mechanisms by which apoptosis inhibition might prevent regeneration, we characterized the pattern of proliferating cells in the regeneration bud using anti-H3P—an antibody that recognizes cells in the G_2/M transition of the cell cycle. This reagent is useful for identifying mitotic cells in regenerating systems including *Xenopus* (Saka and Smith, 2001; Sanchez Alvarado, 2003). Normal regeneration includes an up-regulation of mitosis in and near the growth zone by 48 hpa (Fig. 4A, note increased density of H3P-positive cells near amputation site vs. in more rostral region). In contrast, larvae exposed to apoptosis inhibitor exhibit a drastically reduced number of mitotic cells (Fig. 4B; average of 65 H3P-positive cells in controls vs. 32 in apoptosis-inhibited larvae (SD=9.3, *N*>190, $p<0.01$)). The inhibition of proliferation is not a general (non-specific) effect of M50054: during exposure, embryos continued to grow to the same size as amputated controls (Fig. 2A) and did not exhibit the typical very short and narrow lack-of-growth phenotype observed in embryos in which all cell proliferation was abolished by γ-irradiation (Figs. 4C, C′). Thus, programmed cell death is upstream of the cell proliferation increase in the bud that precedes the rebuilding of the tail; failure to initiate the increase in mitosis is likely to be at least part of the mechanism by which apoptosis inhibition prevents regeneration.

Since apoptosis-inhibited larvae do not regenerate at all, it was impossible to probe for markers normally expressed in the newly regenerating tissue, such as those in the *Notch* pathway (Beck et al., 2003; Slack et al., 2004). To characterize the regeneration bud, we examined the patterns of axon growth in the region at 48 hpa. In control larvae, neuronal projections can be seen extending to the edge of the early regeneration bud and then appear in bundles running parallel to the anterior–posterior axis of the tail (Fig. 4D). In contrast, axons in apoptosis-inhibited larvae (Fig. 4D′) stop at widely varying distances from the end of the bud, with an average distance from uncut neurons to stump tip of 63 μM (*n*=8, SD=36 μM), and are present in tangled bunches often curving perpendicularly to the main axis of the tail. This pattern remains throughout 6 days post-amputation, by which time control tadpoles have regenerated a full tail with axons extending to the distal tip.

Taken together, these data reveal novel roles of caspase-3-mediated apoptosis upstream of the induction of cell proliferation. Some apoptosis is clearly required for normal regeneration (Fig. 2). However, the non-permissive period is associated with a much-expanded region of programmed cell death. The necessity for some apoptosis, together with the excessive cell death present during the non-permissive refractory period, suggests that, like a number of developmental controls (Dyson and Gurdon, 1998; Green, 2002; McDowell and Gurdon, 1999), an intermediate level of caspase-3 activity is required for normal regeneration.

The fact that regeneration fails to take place after apoptotic inhibition in tissues that do not themselves show apoptosis (e.g., the fin edges in Fig. 1C) suggests that tail regeneration in all parts of the tail may depend upon signals from a smaller cell population. Thus, the requirement for apoptosis may be non-cell-autonomous for some cells during regeneration, as has previously been observed in the case of the role of innervation in limb regeneration (Kiba, 2002; Singer, 1952). The fact that the apoptosis we do observe is at the neurogenic component of the bud (e.g., Figs. 1C″, F) is consistent with this, and taken together our data suggest that apoptosis in a medial group of cells is required for a signal that in turn is needed for regeneration of tissues outside that region.

Moreover, apoptosis appears to be required for the normal inhibition of mineralization in the anterior axis and for the proper patterning of neural outgrowths in the regenerate. The existence of apoptosis has been reported in the context of regeneration in planaria (Hwang et al., 2004), *Xenopus* limbs (Suzuki et al., 2005) and newts (Kaneko et al., 1999); however, the above functional data indicate that caspase-3-mediated programmed cell death is an endogenous, required aspect of regeneration in at least one vertebrate. One possibility is that there is a native cellular subpopulation that normally inhibits growth and regeneration, and that it must be destroyed in order for regeneration to take place. Interestingly, the fact that regeneration of tissues that normally do not contain apoptotic cells (e.g., the fin edges in Fig. 1C) is also abrogated following apoptosis inhibition suggests that activation of the highly coordinated regeneration program in many parts of the nascent tail depend upon signals from the region which does contain apoptotic cells. This non-cell-autonomous dependence on apoptosis may be analogous to the well-known requirement for innervation in limb regeneration (Bryant et al., 1971; Singer and Ilan, 1977; Thornton, 1970), and the apoptosis we describe is in fact present in the neurogenic component of the regeneration bud. These findings provide an additional molecular entry point into the investigation of the non-permissive environments that have been observed for nervous system regeneration in mammals (Hirsch and Bahr, 1999; Xiang et al., 2005) and suggest that it would be fruitful to explore selective cell death as a possible mechanism for augmenting regeneration in biomedical contexts.

Acknowledgments

References

Abdel-Karim AE, Michael MI, Anton HJ. Mitotic activity in the blastema and stump tissues of regenerating hind limbs of *Xenopus laevis* larvae after amputation at ankle level. An autoradiographic study. Folia Morphol (Praha). 1990; 38:1–11. [PubMed: 2341072]

Bagri A, Cheng HJ, Yaron A, Pleasure SJ, Tessier-Lavigne M. Stereotyped pruning of long hippocampal axon branches triggered by retraction inducers of the semaphorin family. Cell. 2003; 113:285–299. [PubMed: 12732138]

Bastida MF, Delgado MD, Wang B, Fallon JF, Fernandez-Teran M, Ros MA. Levels of Gli3 repressor correlate with Bmp4 expression and apoptosis during limb development. Dev Dyn. 2004; 231:148–160. [PubMed: 15305295]

Beck CW, Christen B, Slack JM. Molecular pathways needed for regeneration of spinal cord and muscle in a vertebrate. Dev Cell. 2003; 5:429–439. [PubMed: 12967562]

Briegleb W, Neubert J, Schatz A, Klein T, Kruse B. Survey of the vestibulum, and behavior of *Xenopus laevis* larvae developed during a 7-days space flight. Adv Space Res. 1986; 6:151–156. [PubMed: 11537815]

Bryant SV, Fyfe D, Singer M. The effects of denervation on the ultrastructure of young limb regenerates in the newt, *Triturus*. Dev Biol. 1971; 24:577–595. [PubMed: 5578891]

Cadinouche MZ, Liversage RA, Muller W, Tsilfidis C. Molecular cloning of the *Notophthalmus viridescens* radical fringe cDNA and characterization of its expression during forelimb development and adult forelimb regeneration. Dev Dyn. 1999; 214:259–268. [PubMed: 10090152]

Chakraborty C, Nandi SS, Sinha S, Gera VK. Zebrafish caspase-3: molecular cloning, characterization, crystallization and phylogenetic analysis. Prot Peptide Letters. 2006; 13:633–640.

Deuchar EM. Regeneration of the tail bud in *Xenopus* embryos. J Exp Zool. 1975; 192:381–390. [PubMed: 1141840]

Dyson S, Gurdon JB. The interpretation of position in a morphogen gradient as revealed by occupancy of activin receptors. Cell. 1998; 93:557–568. [PubMed: 9604931]

Erdem S, Mendell JR, Sahenk Z. Fate of Schwann cells in CMT1A and HNPP: evidence for apoptosis. J Neuropathol Exp Neurol. 1998; 57:635–642. [PubMed: 9630241]

Frankfurt OS. Decreased stability of DNA in cells treated with alkylating agents. Exp Cell Res. 1990; 191:181–185. [PubMed: 2257876]

Gardiner DM, Endo T, Bryant SV. The molecular basis of amphibian limb regeneration: integrating the old with the new. Semin Cell Dev Biol. 2002; 13:345–352. [PubMed: 12324216]

Gargioli C, Slack JM. Cell lineage tracing during *Xenopus* tail regeneration. Development. 2004; 131:2669–2679. [PubMed: 15148301]

Goltzene F, Skalski M, Wolff CM, Meyer D, Mager-Heckel AM, Darribere T, Remy P. Heterotopic expression of the Xl-Fli transcription factor during *Xenopus* embryogenesis: modification of cell adhesion and engagement in the apoptotic pathway. Exp Cell Res. 2000; 260:233–247. [PubMed: 11035918]

Graham A, Koentges G, Lumsden A. Neural crest apoptosis and the establishment of craniofacial pattern: an honorable death. Mol Cell Neurosci. 1996; 8:76–83.

Green J. Morphogen gradients, positional information, and *Xenopus*: interplay of theory and experiment. Dev Dyn. 2002; 225:392–408. [PubMed: 12454918]

Guha U, Gomes WA, Kobayashi T, Pestell RG, Kessler JA. In vivo evidence that BMP signaling is necessary for apoptosis in the mouse limb. Dev Biol. 2002; 249:108–120. [PubMed: 12217322]

Hirsch S, Bahr M. Growth promoting and inhibitory effects of glial cells in the mammalian nervous system. Adv Exp Med Biol. 1999; 468:199–205. [PubMed: 10635030]

Honig LS, Rosenberg RN. Apoptosis and neurologic disease. Am J Med. 2000; 108:317–330. [PubMed: 11014725]

Huguet C, Morrice DR, Bouali F, Vandenbunder B, Burt DW, Abbadie C. Expression of transcription factor c-Rel and apoptosis occurrence in polydactylous and syndactylous limb buds of the talpid3 mutant chick embryo. Apoptosis. 1999; 4:31–38. [PubMed: 14634293]

Hwang JS, Kobayashi C, Agata K, Ikeo K, Gojobori T. Detection of apoptosis during planarian regeneration by the expression of apoptosis-related genes and TUNEL assay. Gene. 2004; 333:15–25. [PubMed: 15177676]

Ishino T, Shirai M, Kunieda T, Sekimizu K, Natori S, Kubo T. Identification of genes induced in regenerating *Xenopus* tadpole tails by using the differential display method. Dev Dyn. 2003; 226:317–325. [PubMed: 12557209]

James TN. Normal and abnormal consequences of apoptosis in the human heart. From postnatal morphogenesis to paroxysmal arrhythmias Circulation. 1994; 90:556–573.

Johnston MV. Clinical disorders of brain plasticity. Brain Dev. 2004; 26:73–80. [PubMed: 15036425]

Kaneko Y, Matsumoto G, Hanyu Y. The occurrence of apoptosis during retinal regeneration in adult newts. Brain Res Dev Brain Res. 1999; 117:225–228.

Kiba T. The role of the autonomic nervous system in liver regeneration and apoptosis-recent developments. Digestion. 2002; 66:79–88. [PubMed: 12428066]

Lademann U, Cain K, Gyrd-Hansen M, Brown D, Peters D, Jaattela M. Diarylurea compounds inhibit caspase activation by preventing the formation of the active 700-kilodalton apoptosome complex. Mol Cell Biol. 2003; 23:7829–7837. [PubMed: 14560026]

Makino S, Whitehead GG, Lien CL, Kim S, Jhawar P, Kono A, Kawata Y, Keating MT. Heat-shock protein 60 is required for blastema formation and maintenance during regeneration. Proc Natl Acad Sci U S A. 2005; 102:14599–14604. [PubMed: 16204379]

Mallat M, Marin-Teva JL, Cheret C. Phagocytosis in the developing CNS: more than clearing the corpses. Curr Opin Neurobiol. 2005; 15:101–107. [PubMed: 15721751]

McDiarmid, RW.; Altig, R. Tadpoles: The Biology of Anuran Larvae. University of Chicago Press; Chicago, IIL: 1999.

McDowell N, Gurdon JB. Activin as a morphogen in *Xenopus* mesoderm induction. Semin Cell Dev Biol. 1999; 10:311–317. [PubMed: 10441545]

Nagy L, Thomazy VA, Davies PJ. A transgenic mouse model for the study of apoptosis during limb development. Cell Death Differ. 1998; 5:126. [PubMed: 10200453]

Nieuwkoop, PD.; Faber, J. Normal Table of Xenopus laevis (Daudin). North-Holland Publishing Company; Amsterdam: 1967.

Offner N, Duval N, Jamrich M, Durand B. The pro-apoptotic activity of a vertebrate Bar-like homeobox gene plays a key role in patterning the *Xenopus* neural plate by limiting the number of chordin- and shh-expressing cells. Development. 2005; 132:1807–1818. [PubMed: 15772136]

Porter AG, Janicke RU. Emerging roles of caspase-3 in apoptosis. Cell Death Differ. 1999; 6:99–104. [PubMed: 10200555]

Ryffel GU, Werdien D, Turan G, Gerhards A, Goosses S, Senkel S. Tagging muscle cell lineages in development and tail regeneration using Cre recombinase in transgenic *Xenopus*. Nucleic Acids Res. 2003; 31:e44. [PubMed: 12682379]

Saka Y, Smith JC. Spatial and temporal patterns of cell division during early *Xenopus* embryogenesis. Dev Biol. 2001; 229:307–318. [PubMed: 11150237]

Sanchez Alvarado A. The freshwater planarian *Schmidtea mediterranea*: embryogenesis, stem cells and regeneration. Curr Opin Genet Dev. 2003; 13:438–444. [PubMed: 12888018]

Saunders JW Jr. Death in embryonic systems. Science. 1966; 154:604–612. [PubMed: 5332319]

Singer M. The influence of the nerve in regeneration of the amphibian extremity. Q Rev Biol. 1952; 27:169–200. [PubMed: 14949331]

Singer M, Ilan J. Nerve-dependent regulation of absolute rates of protein synthesis in newt limb regenerates. Measurement of methionine specific activity in peptidyl-tRNA of the growing polypeptide chain. Dev Biol. 1977; 57:174–187. [PubMed: 863105]

Sive, HL.; Grainger, RM.; Harland, RM. Early Development of Xenopus laevis. Cold Spring Harbor Laboratory Press; New York: 2000.

Slack JM, Beck CW, Gargioli C, Christen B. Cellular and molecular mechanisms of regeneration in *Xenopus*. Philos Trans R Soc Lond, B Biol Sci. 2004; 359:745–751. [PubMed: 15293801]

Stahelin BJ, Marti U, Solioz M, Zimmermann H, Reichen J. False positive staining in the TUNEL assay to detect apoptosis in liver and intestine is caused by endogenous nucleases and inhibited by diethyl pyrocarbonate. Mol Pathol. 1998; 51:204–208. [PubMed: 9893746]

Streeter GL. Some experiments on the developing ear vesicle of the tadpole with relation to equilibration. J Exp Zool. 1906; 3:543–558.

Sugiura T, Taniguchi Y, Tazaki A, Ueno N, Watanabe K, Mochii M. Differential gene expression between the embryonic tail bud and regenerating larval tail in *Xenopus laevis*. Dev Growth Differ. 2004; 46:97–105. [PubMed: 15008858]

Suzuki M, Satoh A, Ide H, Tamura K. Nerve-dependent and-independent events in blastema formation during *Xenopus* froglet limb regeneration. Dev Biol. 2005; 286:361–375. [PubMed: 16154125]

Thornton CS. Amphibian limb regeneration and its relation to nerves. Am Zool. 1970; 10:113–118. [PubMed: 5426253]

Trindade M, Messenger N, Papin C, Grimmer D, Fairclough L, Tada M, Smith JC. Regulation of apoptosis in the *Xenopus* embryo by Bix3. Development. 2003; 130:4611–4622. [PubMed: 12925588]

Tsuda T, Ohmori Y, Muramatsu H, Hosaka Y, Takiguchi K, Saitoh F, Kato K, Nakayama K, Nakamura N, Nagata S, Mochizuki H. Inhibitory effect of M50054, a novel inhibitor of apoptosis, on anti-Fas-antibody-induced hepatitis and chemotherapy-induced alopecia. Eur J Pharmacol. 2001; 433:37–45. [PubMed: 11755132]

Van Stry M, McLaughlin KA, Ataliotis P, Symes K. The mitochondrial-apoptotic pathway is triggered in *Xenopus* mesoderm cells deprived of PDGF receptor signaling during gastrulation. Dev Biol. 2004; 268:232–242. [PubMed: 15031119]

Xiang S, Pan W, Kastin AJ. Strategies to create a regenerating environment for the injured spinal cord. Curr Pharm Des. 2005; 11:1267–1277. [PubMed: 15853683]

Yang S, Lockwood A, Hollett P, Ford R, Kao K. Overexpression of a novel *Xenopus* rel mRNA gene induces tumors in early embryos. J Biol Chem. 1998; 273:13746–13752. [PubMed: 9593716]

Yu SY, Yoo SJ, Yang L, Zapata C, Srinivasan A, Hay BA, Baker NE. A pathway of signals regulating effector and initiator caspases in the developing *Drosophila* eye. Development. 2002; 129:3269–3278. [PubMed: 12070100]
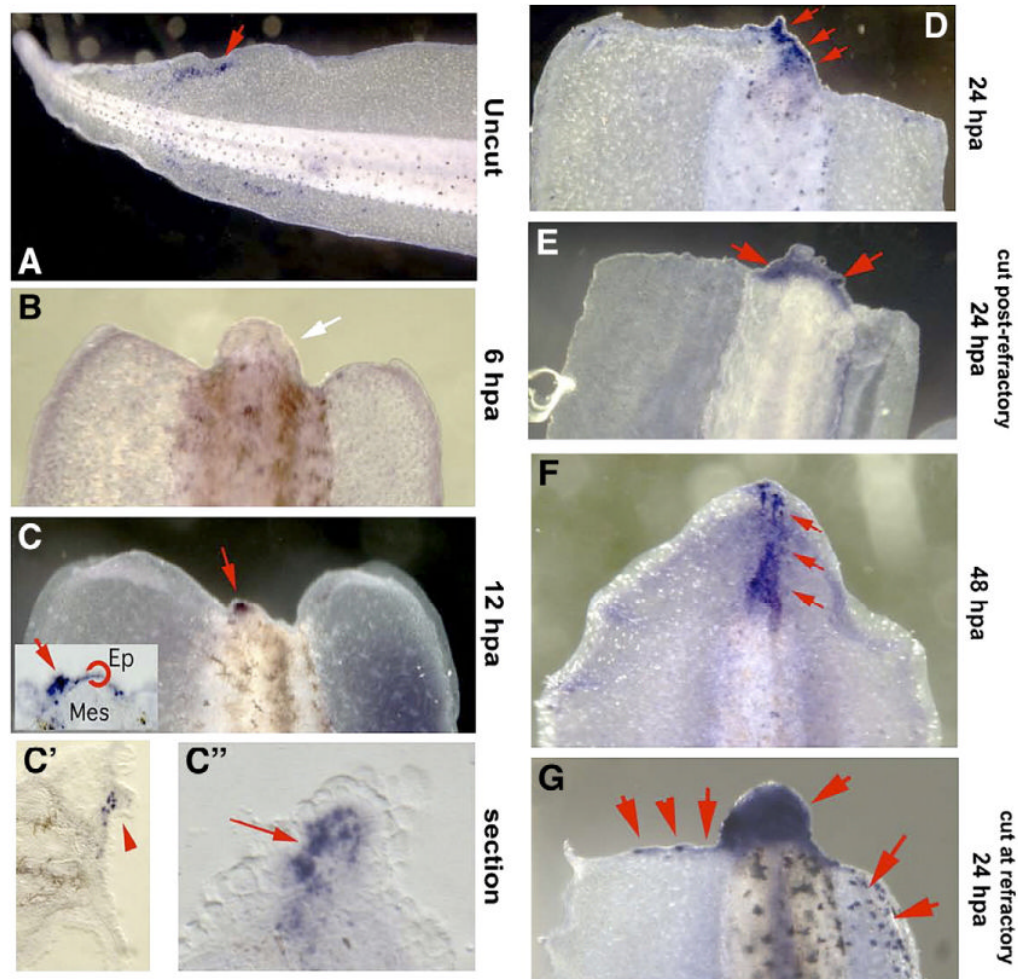
Fig. 1.
Endogenous pattern of apoptosis in *Xenopus* regeneration. Legend: Larvae were processed for immunohistochemistry with an antibody to activated caspase-3, a marker of apoptosis. Positive signals are deep purple. Hpa labels on each panel indicate stage in hours-post-amputation. Larvae in panels B–E were amputated at st. 40; the animal in panel A was not amputated, and that in panel G was amputated during the refractory period (st. 46). (A) Intact larvae at st. 45 possessed small numbers of randomly distributed apoptotic cells; tails at all stages both before and after this period exhibited the same pattern. Red arrowhead indicates one set of positive cells. (B) Six hours post-amputation, no specific signal was detected near the wound swelling. (C) At 12 hpa, a discrete focus of caspase-3-positive cells is located in the nascent regeneration bud (red arrow). Inset: sectioning reveals an epithelial component to the staining that is not obvious in a whole mount, shown also in superficial (C′) and deep (C″) sections that reveal epithelial and mesenchymal caspase-3-positive cells. (D) At 24 hpa, the apoptotic region has expanded (red arrows). (E) When amputation was performed at st. 48 (after the refractory period), tails at 24 hpa likewise exhibit a degree of apoptosis in the bud. (F) At 48 hpa, apoptosis can be detected in cells along the axis (red arrows). (G) In larvae amputated during the refractory period (st. 46), significantly more apoptosis can be detected at 24 hpa-the refractory swelling is almost entirely apoptotic in contrast to the small apoptotic region in regenerating tails, and foci of apoptotic cells can be

seen extending ventrally along the amputation edge border (red arrows). Dorsal is up in panel A; dorsal is to the right in panels B–G.
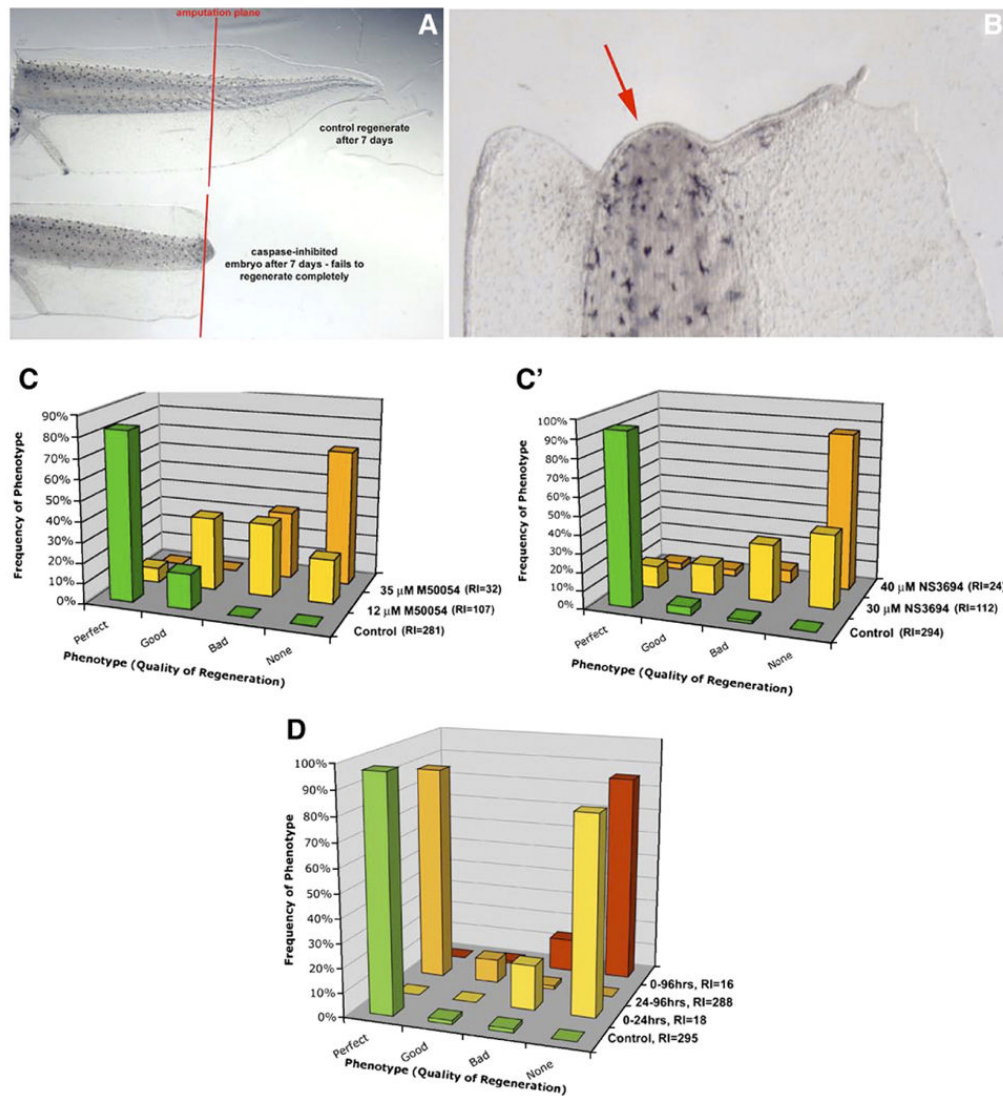
Fig. 2.
Apoptosis is required for regeneration during the first 24 h. Legend: (A) In contrast to control embryos that regenerate a tail within 7 days, larvae treated with a specific apoptosis inhibitor between stages 40 and 46 completely failed to regenerate. (B) Close-up of the amputation site from an inhibited tail, 7 days after amputation. The graphs in panels C and C′ represent averages of replicate experiments performed 3 times each. (C) The effect was concentration dependent: compared to control embryos (regeneration index 281±10), those treated with 12 μM or 35 μM of the inhibitor exhibited regeneration indexes that were 38% and 12% of the controls, respectively. (C′) The same concentration-dependent effect was observed for NS3694, a different apoptosis blocker, significantly reducing the ability of the animals to regenerate: compared to control embryos (regeneration index 294±6), those treated with 12 μM or 35 μM of the inhibitor exhibited regeneration indexes that were 38% and 8% of the controls. (D) This effect was highly time dependent: treatment that lasted only over the first 24 h post-amputation-inhibited regeneration to almost the same degree as inhibition lasting over 7 days, while inhibition that began at 24 h and continued throughout 7 days had no significant effect on regeneration. RI for three replicates combined is noted in the axis labels. Dorsal is to the top in panel A, and to the left in panel B.
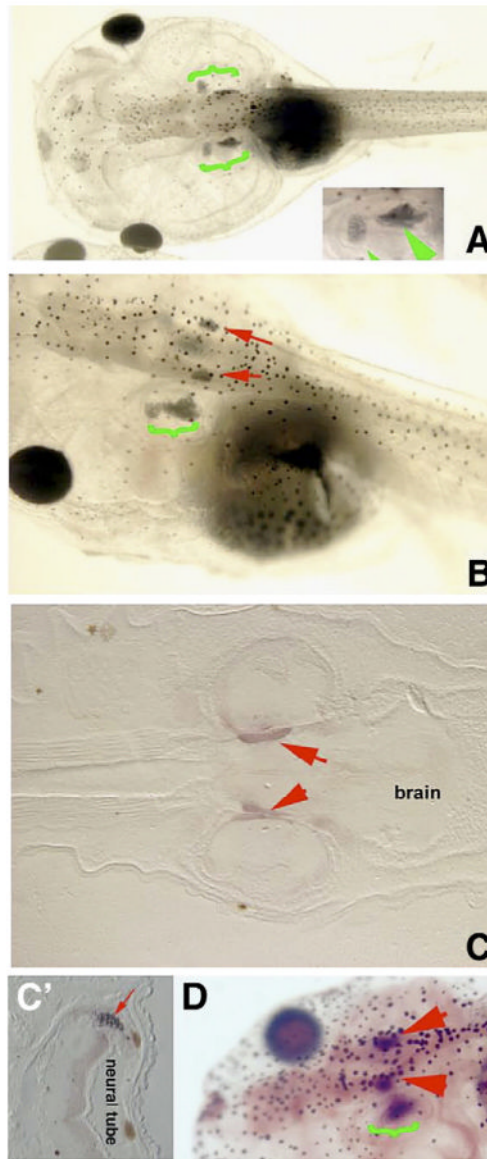
Fig. 3.
Apoptosis inhibition results in ectopic otoliths. Legend: At st. 46, control larvae possess two otoliths that are visible lateral to the neural tube from the dorsal view (A, green brackets, close-up inset). Larvae exposed to apoptosis inhibitor between stages 40 and 46 develop two ectopic otoliths located medial–dorsal and adjacent to the endogenous otoliths (B). (C) Sectioned larva stained for mineralized tissues (red arrows) revealing the ectopic mineralized tissues to be located outside and medial to the otocyst, possibly within brain tissue; normal otoliths occur ventral to the position of the ectopic otoliths and are thus not present in this planar section. (C′) Transverse section showing ectopic otolith (red arrow) next to the neural tube (the two brown circles are melanocytes). (D) Staining for mineralized tissue in whole mount also reveals ectopic otoliths (red arrows) in the hindbrain. Green bracket indicates endogenous otoliths. Red arrowheads indicate ectopic otoliths. Anterior is to the right in panel C, and to the left in panels A, B and D.
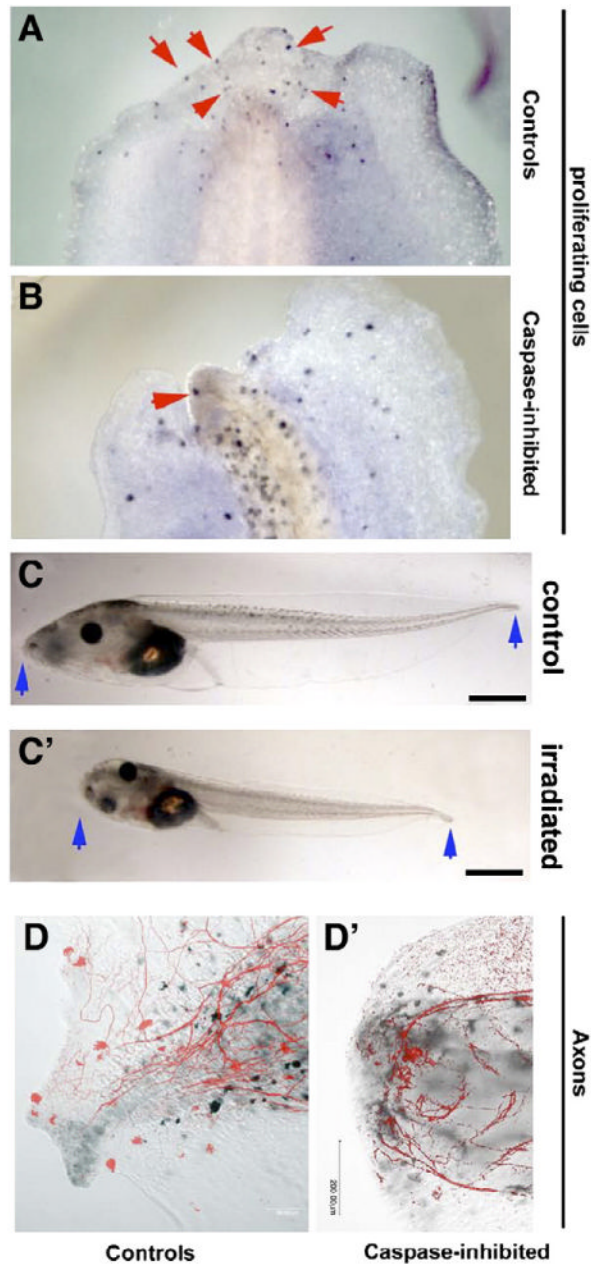
Fig. 4.
Apoptosis inhibition results in inhibition of cell proliferation and neuronal mispatterning near the amputation site. Legend: H3P-positive cells are easily distinguishable from pigment cells by their color (blue vs. brown) and morphology (dendritic melanocytes vs. small round nuclear H3P stain). (A) Control larvae at 48 hpa contain many proliferating cells in the growth region (identified by staining for phosphorylated Histone 3B, a marker of G_2/M transition; four such cells are indicated by red arrowheads; average was 65). (B) In contrast, larvae treated with apoptosis inhibitor have many fewer cells at the G_2/M transition in their growth region (average of 32, SD=9.3, $p<0.01$ compared to controls). When placed side by side with control animals (C), irradiated animals are significantly shorter and narrower (C′); this effect of global reduction of cell proliferation was not observed in drug-treated embryos (compare embryo trunk widths in Fig. 2A), showing that a direct and general inhibition on

cell proliferation was not associated with exposure to apoptosis inhibitors. At 72 hpa, staining for axons reveals the early presence of neurons throughout the regeneration bud. In contrast to control regeneration where axons run parallel to the tail's main axis (D), apoptosis-inhibited larvae's axons do not extend all the way to the end of the regeneration bud and are present in tangles, often curling perpendicular to the main axis (D′). Dorsal is to the left in panels A and B.